Anti-inflammatory effect of Irisin on LPS-stimulated macrophages through inhibition of MAPK pathway

Author: Yuke Ma[1], Yukuan Du[2], Jingnan Yang[2], Qiaoling He[4], Huichao Wang[3], Xuhong Lin[2]

[1]School of Clinical Medicine, Henan University, Kaifeng, China [2]Department of Clinical Laboratory, Huaihe Hospital of Henan University, Kaifeng, China, [3]Department of Nephrology, The First Affiliated Hospital of Henan University, Kaifeng, China, [4]Department of Clinical Laboratory, Wuhan First Hospital, Wuhan, China

Summary

This study aimed to investigate the effect of irisin on LPS-induced inflammation in RAW 264.7 macrophages through inhibition of the mitogen-activated protein kinase (MAPK) pathway. A network pharmacology-based approach, combined with molecular docking and in vitro validation was performed to identify the biological activity, key targets, and potential pharmacological mechanisms of irisin against LPS-induced inflammation. By matching 100 potential genes of irisin with 1893 ulcerative colitis (UC)-related genes, 51 common genes were obtained. Using protein-protein interaction networks (PPI) and component-target network analysis,10 core genes of irisin on UC were further identified. The results of gene ontology (GO) enrichment analysis showed that the molecular mechanisms of irisin on UC were mainly related to mainly enriched in the categories of response to xenobiotic stimulus, response to the drug, and negative regulation of gene expression. Molecular docking results showed good binding activity for almost all core component targets. More importantly, MTT assay and flow cytometry results showed that LPS-induced cytotoxicity was reversed by irisin, after coincubation with irisin, the level of IL-12 and IL-23 decreased in LPS-stimulated RAW264.7 macrophages. Irisin pretreatment significantly inhibited the phosphorylation of ERK and AKT and increased the expression of PPAR α and PPAR γ. LPS-induced enhancement of phagocytosis and cell clearance was reversed by irisin pretreatment. Irisin ameliorated LPS-induced inflammation by inhibiting cytotoxicity and apoptosis, and this protective effect may be mediated through the MAPK pathway. These findings confirm our prediction that irisin plays an anti-inflammatory role in LPS-induced inflammation via the MAPK pathway.

Keywords irisin • LPS • RAW264.7 • MAPK • ERK

Correspondence: Xuhong Lin, Huaihe Hospital of Henan University, 115 Ximen Street, Kaifeng City, Henan Province, China. Email lxh80726@126.com

Introduction

Irisin is cleaved and secreted from the fibronectin type III domain containing 5 (FNDC5) and exerts protective effects against metabolic diseases in humans and mice, and its production is stimulated by exercise and exposure to cold [1, 2]. Irisin is known to protect against metabolic disturbances and stimulates adipocyte transition from white to brown through the MAPK and ERK MAP kinase signaling [3, 4]. There have been a large number of clinical and experimental research reports that irisin is a key factor in the process of pathogenic diseases [5-8]. Recent studies have found that irisin plays an important biological function in other system diseases, such as regulating depression[9], regulates osteoblast proliferation[10], and cortical bone mass [11]. Irisin can also replace ischemic neuronal damage by activating AKT and ERK1/2 signaling pathways [12].

The anti-inflammatory effects of exercise attenuate persistent inflammation-mediated chronic diseases such as type 2 diabetes mellitus (T2DM) and cardiovascular disease (CVD) [13, 14]. It has been reported that exercise is proposed as an auxiliary anti-inflammatory treatment, and physiological movement and inflammatory markers are negatively related [15, 16]. Regular exercise has been shown to reduce systemic chronic inflammation in both longitudinal and cross-sectional studies [17]. Endurance exercise training exerts global anti-inflammatory responses in multiple organs, including skeletal muscle, liver, and adipose tissue through both the reduction of visceral fat mass and the induction of an anti-inflammatory environment with each bout of exercise [18]. A recent study shows that voluntary exercise can attenuate the severity of colonic damage in mice fed with a High-Fat Diet through the release of protective irisin [19]. It has also been shown that exercise can reduce the expression of toll-like receptors (TLRs) and inflammatory signaling [20]. Moderate exercise can produce beneficial ameliorative effects on inflammatory bowel disease (IBD) and improve the healing of colitis in experimental animals due to the activity of protective action, such as irisin released from working skeletal muscle [2]. This was confirmed in Liu's study where voluntary exercise prevented UC [21], which illustrates the anti-inflammatory effect of exercise.

Exercise-induced irisin production has been demonstrated to have protective effects against neuroinflammation [22], mice obesity-induced inflammation [23], and heart hypertrophy [24].

FNDC4 is an anti-inflammatory factor in macrophages and ameliorates induced colitis in a mouse model. FNDC5 as a precursor for irisin synthesis shares high homology with FNDC4 [25]. Therefore, we speculate that irisin may play an important role in the treatment of UC. Visceral adipose tissue (VAT) browning due to irisin's anti-inflammatory effects, which could lead to a reduction in VAT mass [26]. Irisin also decreases inflammation and improves non-alcoholic fatty liver disease by competitive binding with myeloid differentiation factor 2 [20]. Dextran sulfate sodium salt (DSS) -induced colitis produces an inflammation-induced bone loss, while irisin treatment reduces the inflammatory state of the intestine and bone [27]. In our previous in vivo experiments, irisin has been shown to improve inflammation in a mouse model of UC [28], however, the exact mechanism of the anti-inflammatory effect remains unclear.

To study the pharmacology, phytochemistry, and pharmacokinetics of herbal medicines, network pharmacology has been extensively used. Network pharmacology is a versatile approach that integrates pharmacology, bioinformatics, and computer analysis. It can be used to investigate the intricate relationships in herbal medicines [29]. In reality, network pharmacology generally follows three paths: building a research network based on databases, network analysis to look for important chemicals and targets, and experimental validation to confirm the accuracy of the results [30]. The combination of network pharmacology and experimental validation has emerged as a preferred strategy to explore the core targets and mechanisms of chemicals [31]. In the current study, network pharmacology was utilized to screen a large number of potential targets and anticipate potential signaling pathways to forecast the mechanisms of irisin. Additionally, an in vitro experiment was set up to confirm irisin's ability to reduce inflammation and the core gene's altered expression.

Methods

Prediction of targets related to irisin and UC

First, we obtained the molecular structures and canonical SMILES codes for all components from PubChem (https://pubchem.ncbi.nlm.nih.gov/) [32]. Next, the composition of corresponding targets was collected by using the Swiss Target Prediction (http://www.swisstargetprediction.ch/, ver. 2019) database [33]. Targets related to UC were obtained from two databases aiming to elucidate the relationship between targets and diseases from different perspectives. GeneCards

(https://www.genecards.org/) [34], and DisGeNET (http://www.disgenet.org/) [35] databases were searched with “Ulcerative Colitis” as a keyword. To ensure the reliability of target prediction, we selected disease genes from DisGeNET and selected targets with a correlation score ≥3 in GeneCards. Upload the above-obtained drug and disease genes to Bioinformatics (http://www.bioinformatics.com.cn) to obtain the intersecting genes.

Component-target (C-T) and PPI Network Construction

To understand the complex interactions between components and their corresponding targets, a C-T network was established by using Cytoscape (https://cytoscape.org/, version 3.9.1) [36]. In addition, candidate targets were uploaded to the STRING database (https://string-db.org/, version 11.0) [37] to obtain PPI data by limiting the species to "Homo sapiens". After obtaining PPI data, PPI networks were constructed by Cytoscape. In addition, the degree values of the nodes in the network were calculated and the targets with degree values higher than the median were selected as the key targets of the PPI network.

GO Functional Enrichment Analysis

To investigate the potential molecular mechanisms of irisin on UC, candidate targets were analyzed for GO function enrichment analysis through the DAVID database (https://david.ncifcrf.gov) [38]. The enrichment P-value was calculated, and a $P < 0.05$ was considered to be statistically significant.

Molecular Docking

First, the 2D structure of irisin was downloaded from PubChem and stored in PDB file format, water was removed using PyMOL and then converted to MOL2 files using Open Babel 3.1.1. The structure of the receptor was obtained from the PDB database [39]. Then, the components and target proteins for docking were prepared using PyMOL 1.7.2.1 and saved as PDBQT files using AutoDockTools 1.5.6 [40]. Finally, docking simulations were performed under the AutoDock program and the fraction target with lower affinity scores was selected for further analysis.

Macrophage cell culture

RAW264.7 macrophages were cultured in Dulbecco's Modified Eagle's Medium (DMEM; Corning, USA) containing 10% fetal bovine serum (FBS; Corning, USA) and 1% penicillin/streptomycin (Invitrogen, USA), in 37°C, 5% CO_2 incubator.

Cell MTT test

Cell viability was tested by MTT assay, and 1 x 10^5 cells were seeded in a 96-well plate. After incubation for 24h, treated with various concentrations of LPS (Sigma, USA) (100, 500, 1000, 2000ng/ml) and irisin (400ng/ml) (Phoenix Pharmaceuticals, Inc) for 24h. Then, 20 μl of 5% MTT (Solarbio, USA) solution was added to each well and incubated for 4 h. The supernatant was discarded and the resulting crystals were dissolved in DMSO (Solarbio, USA). Subsequently, the cells were further incubated (37 °C, 5% CO_2) for 10 min. Absorbance was measured at 490nm.

Cell morphology

RAW264.7 was cultured in 12-well plates at 1 × 10^5 cells/well. After incubation for 24h, cells were cultured with medium, irisin (400ng/ml), and LPS (1000ng/ml), respectively, or cells were pretreated with irisin for 12 hours, and then LPS was added. Cell morphology was evaluated with light microscopy.

IL-12 and IL-23 levels

The levels of IL-12 and IL-23 in the supernatants of the four groups of cells were taken and detected by Enzyme-Linked Immunosorbent Assay Kits (ELISA) (Hermes Criterion Biotechnology, Canada), respectively.

Macrophage phagocytosis test

The cell suspension concentration of log-phase RAW264.7 was adjusted to about 1 × 10^5/mL and added 500 μL into each well of the 24-well plate in a 5% CO_2 incubator for 24h at 37°C. Zymosan particles (Invitrogen, USA) were added to the cells. Phagocytosis was allowed to proceed for 30min. Cells were fixed with 4% paraformaldehyde for 30min at 4°C, then washed with PBS. The plate was examined by light microscopy at 400magnification using a Nikon Eclipse Ti2-E microscope (Nikon, Tokyo, Japan). Phagocytosis was determined by counting a total of 100 macrophages in at

least four different fields in 400 magnification photomicrographs. Phagocytosis was assessed as the percentage of phagocytic cells (PP), mean of particles per cell (MNP), and the phagocytic index (PI) determined as PI =PP x MNP.

Western Blot

The total proteins in each group were extracted with RIPA (Solar bio, China), PMSF (Solar bio, China), and Protein Phosphatase Inhibitor (Solar bio, China). The total protein was quantified by the BCA protein assay kit (Beyotime, China), and the protein was denatured at 95℃ for 5min. After electrophoresis, proteins were transferred onto polyvinylidene difluoride (PVDF) (Immobilon, Germany), followed by 5% non-fat milk（Solarbio, China）to block the band. The band was then incubated with primary antibody (β-actin, Proteintech, China, Mouse, 1:5000, ERK1/2, Proteintech, China, Rabbit, 1:1000; Phospho-ERK1/2, Proteintech, China, Rabbit, 1:1000; AKT, Proteintech, China, Mouse, 1:2000; Phospho-AKT, Proteintech, China, Rabbit, 1:5000; PPAR α， Proteintech, China, Mouse, 1:1000; PPAR γ， Proteintech, China, Rabbit, 1:1000) at 4°C overnight, the appropriate secondary antibody HRP-conjugated affinity purified goat anti-rabbit, or goat anti-mouse IgG was applied at 1:5000 dilution and incubated for 1 hour at room temperature. Images were taken with a Bio-Rad imaging system (Bio-Rad, USA) and analyzed by an image analysis system for the optical density of the protein bands.

Flow Cytometry

To compare the apoptosis rate, RAW264.7 macrophages were divided into four groups, treated with culture medium, irisin (400 ng/ml), LPS (1000 ng/ml) alone, pretreated with irisin, and then added with LPS. In addition, to assess the apoptotic rate of thymocytes, thymocytes and supernatants were collected after thymocytes were treated with dexamethasone (5 μM) (Yeasen, China) for 12 hours. then, centrifuged at 3000 r/min for 5 minutes, and resuspended in 500 μL Binding Buffer. Annexin V-FITC and PI (Procell, China) were added with 5 μL respectively, and flow cytometry quantitative detection was performed with FACS.

Apoptotic Cell Clearance Assay

Macrophages were seeded in 24-well plates. Apoptotic thymocytes were added to each well at a

macrophage: thymocyte ratio of (1:10). Thymocytes were labeled with fluorescent cell tracking reagent (Invitrogen, USA) before co-culture with macrophages. Phagocytosis assays were performed at 37°C for 1 hour. Macrophages were then washed thoroughly to remove non-phagocytic cells. Fix cells with 4% paraformaldehyde. Image analysis was performed by a fluorescence microscope (thymocytes, red). Quantify thymocytes phagocytosed by each macrophage using Image J by counting 50-100 macrophages in each well. Data are presented as phagocytosis index. This index was defined as the total number of apoptotic cells phagocytosed by each macrophage present in the field of view.

Statistical analysis

Results were expressed as mean ± SE, all data were tested for normality by using Prism 9.0 software (GraphPad Software), using one-way ANOVA if they conformed to a normal distribution, otherwise using the Kruskal-Wallis test. P-values <0.05 were considered statistically significant.

Results

Candidate targets and PPI network construction

A total of 100 potential targets for irisin were identified from the Swiss target prediction database by uploading the 2D structure of irisin (Figure 1 (A)). Also, 1,893 UC-related targets were obtained from the Gene Cards and DisGeNET databases after eliminating duplicates. Interestingly, after Venn diagram analysis, we found that 51 irisin-related targets were included in the UC (Figure 1 (B)), Table S1). Additionally, the above targets were used to construct a PPI network with the String database. The PPI network included 51 nodes and 293 edges (Figure 1 (C), Table S2). Then, the network was imported into Cytoscape software and analyzed with the Network Analyzer tool (Figure 1 (D)). A thicker edge indicated a higher combined score, while a deeper node color and larger size indicated a higher degree of interaction.

GO enrichment analyses

To investigate the potential mechanism of irisin action on UC, GO enrichment analysis was performed on 51 cross-targets using the DAVID database (https://david.ncifcrf. gov). GO analyzes the target gene function at three levels: cellular component (CC), molecular function (MF), and

biological process (BP). Finally, based on a P-value of < 0.05, the top 20 significantly enriched BP, CC, and MF terms were selected to construct a bar graph (Figure 1 (E)). As shown in Figure 1E (Table S3), the BP domain was mainly enriched in the categories of response to xenobiotic stimulus, response to drug, negative regulation of gene expression, angiogenesis, positive regulation of ERK1 and ERK2 cascade, and positive regulation of MAPK cascade. The CC domain was mainly enriched in the categories of the plasma membrane, cytosol, cytoplasm, extracellular region, extracellular space, and extracellular exosome. The MF domain was mainly enriched in the categories of zinc ion binding, protein kinase activity, enzyme binding endopeptidase activity, and serine-type endopeptidase activity.

C-T Network Analysis

The top 10 hub targets of the PPI network were identified using the EPC algorithm of the cytoHubba plugin of Cytoscape software. In general, the hub targets ranked from highest to lowest were MAP kinase p38 alpha (MAPK14), Arachidonate 5-lipoxygenase (ALOX5), and Thymidine phosphorylase (TYMP), Transforming protein p21/H-Ras-1 (HRAS) and Peroxisome proliferator-activated receptor gamma (PPAR γ) (Figure 1 (F), Table S4). A chemical-target-specific phenotypic network map was constructed using Cytoscape software to demonstrate the relationship between irisin and UC.

Docking Results Analysis

According to the PPI and Cytoscape analyses, two candidate target proteins, including PPAR γ (PDB ID: 2znq) and MAPK14 (PDB ID: 5eti), were conducted molecular docking with irisin. The docking score represents the stability of the protein and compound-the lower the score, the stronger the bond. The results revealed that PPAR γ interacted with irisin, as shown in Figure 2 (A-B). As shown in Figure 2A, the structure of quercetin could interact with ARG415, LYS212, and ASP210 through 1 hydrogen bond, respectively. The results indicated that MAPK14 interacted with irisin, as shown in Figure 2 (C-D), the structure of irisin could form one hydrogen bond with ALA306, and HIS312, respectively. A lower docking score represents a more stable binding of the protein and compound [41]. The energy of PPAR γ and MAPK14 docking irisin was (1.32 kcal/mol) and (-0.33 kcal/mol), respectively, and the results indicate that irisin has a good binding activity to PPAR γ and

MAPK14.

Irisin Protected LPS-Induced Cell Injury

We first plated RAW264.7 macrophages into 96-well plates, added different concentrations of LPS (0, 100, 500, 1000, 2000ng/mL), and used an MTT assay to measure cell viability after 24 hours. LPS decreased cell viability in a dose-dependent manner compared to the control group. LPS significantly increased the percentage of apoptotic macrophages at a dose of 1000ng/ml ($P<0.01$) (Figure 3 (A)). The elevated percentage of apoptotic macrophages was reversed by pretreatment with irisin at the concentration of 400ng/ml ($P<0.01$) (Figure 3 (B)). This observation was consistent with flow cytometry results and allowed us to comprehensively assess overall cell viability (Figure 3 (C)).

Irisin changes the morphology of macrophages

To study the impact of irisin on the cell morphology of RAW264.7 macrophages, we observed the alteration of cell morphology under an optical microscope after being treated with medium, irisin, and LPS respectively. After 24h culture, the cell morphology changed significantly. The original shape of RAW264.7 was round. After LPS treatment, the cells were severely differentiated, and irisin pretreatment could improve the cell shape (Figure 3 (D)).

Irisin Inhibited LPS-Induced change of protein

As shown in Figure 4 (A-B), irisin or LPS alone didn't change the expression of ERK, and AKT. Irisin pretreatment significantly abolished LPS-induced phosphorylation of ERK ($P<0.0001$) and also reduced phosphorylation of AKT ($P<0.001$). Consistently, the expression of PPAR α ($P<0.001$) and PPAR γ ($P<0.0001$) is also increased in the irisin group (Figure 4 (C)).

Irisin decreased IL-12 and IL-23 levels induced by LPS

We found that irisin can significantly decrease the elevated level of inflammatory factors in each group caused by LPS (Figure 4 (D)). There was no significant difference in IL-12 and IL-23 levels between the control (11.2 ± 42.1 and 564.2 ± 35.8pg/ml) and irisin (114.4 ± 72.4 and 628.9 ± 77.1pg/ml, respectively) groups. However, the levels of IL-12 (224.7 ± 168.0) and IL-23 (917.5 ±

42.69pg/ml) (P<0.05) were significantly increased in the LPS group compared with the control group. Irisin significantly reduced LPS-mediated upregulation of IL-12 (123.4 ± 73.43pg/ml) and IL-23 (579.8 ± 82.2pg/ml) (P<0.05), but the decrease of IL-12 was not significant.

LPS enhances zymosan phagocytosis

Phagocytosis is a basic immune response reflecting the immune status of the body[42]. Compared with the control group, the irisin-alone culture was unchanged, and its PI was 3.22 ± 0.23. LPS treatment increased phagocytosis efficiency, with PI increasing from 2.68 ± 0.06 in cells cultured in medium only to 5.07 ± 0.13 in cells cultured with LPS 1000ng/ml (P<0.05) (Figure 5(A)). After LPS treatment, the uptake of the zymosan in macrophages was gradually increased, while after irisin pretreatment, its PI was 3.58 ± 0.08 (P<0.05), which greatly reduced this effect.

LPS enhances cell clearance

Over 90% of cells become phosphatidylserine positive after incubation with 5μM dexamethasone. (Figure 5 (B)) The fluorescent-labeled apoptotic cells were engulfed by macrophages. Cells cultured in medium or irisin alone had little effect on apoptotic thymocyte ingestion (PI 0.94 ± 0.02 and PI 1.03 ± 0.04, respectively), whereas LPS significantly enhanced apoptotic thymocyte ingestion (PI 2.28 ± 0.04) (P<0.05) (Figure 5 (C-D)), irisin pretreatment alleviated ingestion (PI 1.12 ± 0.05) (P<0.05).

Discussion

Irisin is a myokine that has been widely explored in recent years. Numerous research found that irisin plays a protective role in metabolic diseases such as diabetes and obesity, and insulin resistance [43-45], moreover, irisin has a role in nervous system disease, including neuronal injury[12], Alzheimer's disease [46], besides, irisin has anti-inflammatory properties in bone turnover changes [47], obese [23], gut [27]. Exercise can exert its anti-inflammatory effects through an anti-inflammatory environment mediated by myokines [48]. The anti-inflammatory effects of exercise may be attributed to the release of irisin [2], which has been shown to attenuate the inflammatory response in a mouse model of UC by altering the intestinal microbiota [28]. The FNDC4 protein, which shares 57% homology with FNDC5, is an anti-inflammatory factor in

macrophages and ameliorates colitis in mice [25]. However, there is still little evidence to explain the effect of irisin on LPS-induced inflammation in vitro. Therefore, it is of great significance to study the anti-inflammatory mechanism of irisin.

In the current study, network pharmacy analysis was used to explore the mechanisms underlying irisin eliminating the LPS-induced inflammation, and the results were experimentally verified in vitro using RAW264.7 macrophages. Overall, network pharmacology analysis identified 51 irisin-related targets included in the UC. Furthermore, the PPI network showed that the relationship between targets is intricate. By exploring the core targets of irisin in UC using the EPC algorithm, the top 5 central targets identified included MAPK14, ALOX5, TYMP, HRAS, and PPAR γ. Among them, MAPK14, associated with the largest number of target nodes in the core PPI network, could be the most important target in irisin against UC. MAPK14 is closely associated with many chronic inflammatory conditions, including UC, which overproduces inflammatory mediators. Macrophage-derived MAPK is thought to be involved in autophagic regulation and inflammatory responses[49]. In addition to MAPK14, we found that PPAR γ associated with more core ingredients in the PPI network. PPAR γ is a target for regulating pro-inflammatory cytokine expression by interfering with NF-κ B and activin-1 gene expression [50-52]. The agonist of PPAR γ plays an anti-inflammatory role in several diseases [53]. In addition, voluntary exercise greatly increased the colonic expression and activity of PPAR γ in HFD and control animals, and these beneficial effects induced by voluntary exercise were abolished by PPAR γ inhibitors [54]. Activation of PPAR γ has been demonstrated to inhibit colonic inflammation in UC or animal models of UC [55], which is mediated by the production of intestinal glucocorticoid [21]. The PPAR α signaling in the anti-inflammatory activity of glucocorticoids modulated and improved the anti-inflammatory response in IBD murine [56]. There was a positive effect of rSj16 on DSS-induced colitis by diminishing pro-inflammatory cytokine production and upregulating immunoregulatory cytokine production [57], which was mediated by PPARα pathway inhibition. Studies have revealed that PPAR is increased at the mRNA level by irisin treatment [1]. In addition, molecular docking was performed to further validate the predicted results of the network pharmacological analysis. The docking results showed that irisin could combine well with MAPK14 and PPAR γ, respectively. This is consistent with our results showing that the expression of PPARα and PPAR γ was decreased after LPS treatment, whereas the expression was increased after irisin pretreatment, indicating that

irisin has a therapeutic effect on LPS-induced macrophage inflammation, which may be related to the increased in PPAR expression.

Lipopolysaccharide (LPS) is a component of the outer membrane of gram-negative bacteria which provides a persistent inflammatory stimulus that produces proinflammatory cytokines [58]. LPS induces an inflammatory response and even death in RAW264.7 macrophages [59]. The expression of IL-12 p70, IL-23, and IL-12 p40 was upregulated by LPS treatment [60]. Previous research has shown that the expression of IL-12 and IL-23 is mediated by MAPK signaling pathways [61, 62]. In our study, LPS increased the expression of IL-12 p40 and IL-23, whereas irisin reversed this effect.

PI3K-dependent AKT phosphorylation is an early event in UC inflammatory signaling [63, 64]. The PI3K/AKT signal transduction pathway is involved in reducing the release of cytokines, reducing the inflammatory response, and playing an important role in the occurrence and development of UC [65]. Irisin pretreatment significantly inhibited the phosphorylation of AKT and increased the expression of PPAR α and PPAR γ. Therefore, it is speculated that the therapeutic effect of irisin on inflammation may be related to the increase of PPAR and PI3K/AKT.

MAPK is a family of serine-threonine kinases involved in various cellular activities, including cell proliferation and apoptosis, including the JNK, ERK, and p38 pathways [66]. Targeting the MAPK signaling pathway may treat inflammatory diseases, as MAPK is active in the inflammatory response by regulating inflammatory cytokines [67]. Activation of the MAPK signaling pathway is considered to be one of the main factors leading to the release of cytokines and inflammatory mediators in ulcerative colitis [68]. MAPK/ERK and PI3K/AKT pathways are upregulated in ulcerative colitis-associated colon cancer [69]. Elevated p ERK is observed in a DSS-induced mouse model of UC, suggesting that MAPK signaling is involved in the development of UC [70]. Activation of AKT and ERK enhances protective defenses against oxidative stress and inflammation in colitis [71]. This is consistent with our findings that the phosphorylation of ERK was decreased after pretreatment with irisin, suggesting that the therapeutic effect of irisin on LPS-induced macrophage inflammation may be associated with increased ERK expression.

Conclusion

The present study showed that irisin can modulate the activation of the MAPK pathway, as

irisin pretreatment significantly inhibited the phosphorylation of ERK and AKT and increased the expression of PPAR α and PPAR γ, LPS promotes inflammation and apoptosis in macrophage RAW264.7, whereas irisin ameliorates this, as validated by flow cytometry and MTT. This study demonstrates that LPS induces inflammation in macrophages and that irisin has beneficial and anti-inflammatory properties for the development of inflammation-related diseases. This effect may be mediated by the MAPK signaling pathway, and further research is needed to block the proteins associated with the signaling pathway.

Conflicts of interest. All authors have no financial interests or potential conflicts of interest to declare.

Acknowledgments. This work was supported partly by grants from Projects supported by the National Natural Science Foundation of China (81500430, U1304802) and the Science and Technology Planning Project to Henan Province (192102310045) to Xuhong Lin, Medical science and Technology Project of Henan Province (2018020320) to Huichao Wang.

Author contribution. All authors contributed to the study's conception and design. Xuhong Lin, Yukuan Du, Huichao Wang, Jingnan Yang, and Yuke Ma collected samples and clinical information. Data were analyzed by Jingnan Yang and Huichao Wang. Qiaoling He and Yukuan Du analyzed and interpreted the data. The first draft of the manuscript was written by Yuke Ma. Xuhong Lin and Yuke Ma revised the manuscript. All authors had full access to the final version of the report and agreed to the submission.

References

1.Bostrom P, Wu J, Jedrychowski MP, Korde A, Ye L, Lo JC, Rasbach KA, Bostrom EA, Choi JH, Long JZ, Kajimura S, Zingaretti MC, Vind BF, Tu H, Cinti S, Hojlund K, Gygi SP, Spiegelman BM. A PGC1-alpha-dependent myokine that drives brown-fat-like development of white fat and thermogenesis. Nature 2012; 481:463-468.

2.Bilski J, Mazur-Bialy A, Brzozowski B, Magierowski M, Zahradnik-Bilska J, Wojcik D, Magierowska K, Kwiecien S, Mach T, Brzozowski T. Can exercise affect the course of inflammatory bowel disease? Experimental and clinical evidence. Pharmacol Rep 2016; 68:827-836.

3.Zhang Y, Li R, Meng Y, Li S, Donelan W, Zhao Y, Qi L, Zhang M, Wang X, Cui T, Yang LJ, Tang

D. Irisin stimulates browning of white adipocytes through mitogen-activated protein kinase p38 MAP kinase and ERK MAP kinase signaling. Diabetes 2014; 63:514-525.
4.Perakakis N, Triantafyllou GA, Fernandez-Real JM, Huh JY, Park KH, Seufert J, Mantzoros CS. Physiology and role of irisin in glucose homeostasis. Nat Rev Endocrinol 2017; 13:324-337.
5.Boström PA, Fernández-Real JM. Metabolism: Irisin, the metabolic syndrome and follistatin in humans. Nature reviews Endocrinology 2014; 10:11-12.
6.Huh JY, Mantzoros CS. Irisin physiology, oxidative stress, and thyroid dysfunction: What next? Metabolism: clinical and experimental 2015; 64:765-767.
7.Qiu S, Cai X, Yin H, Zügel M, Sun Z, Steinacker JM, Schumann U. Association between circulating irisin and insulin resistance in non-diabetic adults: A meta-analysis. Metabolism: clinical and experimental 2016; 65:825-834.
8.Polyzos SA, Mathew H, Mantzoros CS. Irisin: A true, circulating hormone. Metabolism: clinical and experimental 2015; 64:1611-1618.
9.Wang S, Pan J. Irisin ameliorates depressive-like behaviors in rats by regulating energy metabolism. Biochemical and biophysical research communications 2016; 474:22-28.
10.Qiao X, Qiao XY, Nie Y, Ma Y, Ma YX, Chen Y, Cheng R, Yin W, Yinrg WY, Hu Y, Xu W, Xu WM, Xu L, Xu LZ. Irisin promotes osteoblast proliferation and differentiation via activating the MAP kinase signaling pathways. Scientific reports 2016; 6:18732.
11.Colaianni G, Cuscito C, Mongelli T, Pignataro P, Buccoliero C, Liu P, Lu P, Sartini L, Comite MD, Mori G, Benedetto AD, Brunetti G, Yuen T, Sun L, Reseland JE, Colucci S, New MI, Zaidi M, Cinti S, Grano M. The myokine irisin increases cortical bone mass. Proceedings of the National Academy of Sciences of the United States of America 2015; 112:12157-12162.
12.Li DJ, Li YH, Yuan HB, Qu LF, Wang P. The novel exercise-induced hormone irisin protects against neuronal injury via activation of the Akt and ERK1/2 signaling pathways and contributes to the neuroprotection of physical exercise in cerebral ischemia. Metabolism 2017; 68:31-42.
13.Metsios GS, Moe RH, Kitas GD. Exercise and inflammation. Best Pract Res Clin Rheumatol 2020; 34:101504.
14.Pedersen BK. Anti-inflammatory effects of exercise: role in diabetes and cardiovascular disease. Eur J Clin Invest 2017; 47:600-611.
15.Hamer M, Sabia S, Batty GD, Shipley MJ, Tabák AG, Singh-Manoux A, Kivimaki M. Physical activity and inflammatory markers over 10 years: follow-up in men and women from the Whitehall II cohort study. Circulation 2012; 126:928-933.
16.Rana JS, Arsenault BJ, Després J-P, Côté M, Talmud PJ, Ninio E, Jukema JW, Wareham NJ, Kastelein JJP, Khaw K-T, Boekholdt SM. Inflammatory biomarkers, physical activity, waist circumference, and risk of future coronary heart disease in healthy men and women. European heart journal 2011; 32:336-344.
17.Karstoft K, Pedersen BK. Exercise and type 2 diabetes: focus on metabolism and inflammation. Immunol Cell Biol 2016; 94:146-150.
18.Goh J, Goh KP, Abbasi A. Exercise and Adipose Tissue Macrophages: New Frontiers in Obesity Research? Front Endocrinol (Lausanne) 2016; 7:65.
19.Mazur-Bialy AI, Bilski J, Wojcik D, Brzozowski B, Surmiak M, Hubalewska-Mazgaj M, Chmura A, Magierowski M, Magierowska K, Mach T, Brzozowski T. Beneficial Effect of Voluntary Exercise on Experimental Colitis in Mice Fed a High-Fat Diet: The Role of Irisin, Adiponectin and Proinflammatory Biomarkers. Nutrients 2017; 9.

20.Zhu W, Sahar NE, Javaid HMA, Pak ES, Liang G, Wang Y, Ha H, Huh JY. Exercise-Induced Irisin Decreases Inflammation and Improves NAFLD by Competitive Binding with MD2. Cells 2021; 10.
21.Liu WX, Zhou F, Wang Y, Wang T, Xing JW, Zhang S, Sang LX, Gu SZ, Wang HL. Voluntary exercise protects against ulcerative colitis by up-regulating glucocorticoid-mediated PPAR-gamma activity in the colon in mice. Acta Physiol (Oxf) 2015; 215:24-36.
22.Pignataro P, Dicarlo M, Zerlotin R, Zecca C, Dell'Abate MT, Buccoliero C, Logroscino G, Colucci S, Grano M. FNDC5/Irisin System in Neuroinflammation and Neurodegenerative Diseases: Update and Novel Perspective. Int J Mol Sci 2021; 22.
23.Lu Y, Li G. Auricular acupuncture induces FNDC5/irisin and attenuates obese inflammation in mice. Acupunct Med 2020; 38:264-271.
24.Geng Z, Fan WY, Zhou B, Ye C, Tong Y, Zhou YB, Xiong XQ. FNDC5 attenuates obesity-induced cardiac hypertrophy by inactivating JAK2/STAT3-associated inflammation and oxidative stress. J Transl Med 2019; 17:107.
25.Bosma M, Gerling M, Pasto J, Georgiadi A, Graham E, Shilkova O, Iwata Y, Almer S, Soderman J, Toftgard R, Wermeling F, Bostrom EA, Bostrom PA. FNDC4 acts as an anti-inflammatory factor on macrophages and improves colitis in mice. Nat Commun 2016; 7:11314.
26.Gonzalez-Gil AM, Elizondo-Montemayor L. The Role of Exercise in the Interplay between Myokines, Hepatokines, Osteokines, Adipokines, and Modulation of Inflammation for Energy Substrate Redistribution and Fat Mass Loss: A Review. Nutrients 2020; 12.
27.Metzger CE, Narayanan SA, Elizondo JP, Carter AM, Zawieja DC, Hogan HA, Bloomfield SA. DSS-induced colitis produces inflammation-induced bone loss while irisin treatment mitigates the inflammatory state in both gut and bone. Sci Rep 2019; 9:15144.
28.Huangfu LX, Cai XT, Yang JN, Wang HC, Li YX, Dai ZF, Yang RL, Lin XH. Irisin attenuates inflammation in a mouse model of ulcerative colitis by altering the intestinal microbiota. Exp Ther Med 2021; 22:1433.
29.Li QF, Lu WT, Zhang Q, Zhao YD, Wu CY, Zhou HF. Proprietary Medicines Containing Bupleurum chinense DC. (Chaihu) for Depression: Network Meta-Analysis and Network Pharmacology Prediction. Front Pharmacol 2022; 13:773537.
30.Liu J, Liu J, Tong X, Peng W, Wei S, Sun T, Wang Y, Zhang B, Li W. Network Pharmacology Prediction and Molecular Docking-Based Strategy to Discover the Potential Pharmacological Mechanism of Huai Hua San Against Ulcerative Colitis. Drug Des Devel Ther 2021; 15:3255-3276.
31.Li J, Bi H. The effect and mechanism of cypermethrin-induced hippocampal neurotoxicity as determined by network pharmacology analysis and experimental validation. Bioengineered 2021; 12:9279-9289.
32.Kim S, Chen J, Cheng T, Gindulyte A, He J, He S, Li Q, Shoemaker BA, Thiessen PA, Yu B, Zaslavsky L, Zhang J, Bolton EE. PubChem 2019 update: improved access to chemical data. Nucleic acids research 2019; 47:D1102-D1109.
33.Daina A, Michielin O, Zoete V. SwissTargetPrediction: updated data and new features for efficient prediction of protein targets of small molecules. Nucleic acids research 2019; 47:W357-W364.
34.Stelzer G, Rosen N, Plaschkes I, Zimmerman S, Twik M, Fishilevich S, Stein TI, Nudel R, Lieder I, Mazor Y, Kaplan S, Dahary D, Warshawsky D, Guan-Golan Y, Kohn A, Rappaport N, Safran M, Lancet D. The GeneCards Suite: From Gene Data Mining to Disease Genome Sequence Analyses.

Current protocols in bioinformatics 2016; 54:1.30.31-31.30.33.
35.Piñero J, Ramírez-Anguita JM, Saüch-Pitarch J, Ronzano F, Centeno E, Sanz F, Furlong LI. The DisGeNET knowledge platform for disease genomics: 2019 update. Nucleic acids research 2020; 48:D845-D855.
36.Franz M, Lopes CT, Huck G, Dong Y, Sumer O, Bader GD. Cytoscape.js: a graph theory library for visualisation and analysis. Bioinformatics (Oxford, England) 2016; 32:309-311.
37.Szklarczyk D, Gable AL, Lyon D, Junge A, Wyder S, Huerta-Cepas J, Simonovic M, Doncheva NT, Morris JH, Bork P, Jensen LJ, Mering Cv. STRING v11: protein-protein association networks with increased coverage, supporting functional discovery in genome-wide experimental datasets. Nucleic acids research 2019; 47:D607-D613.
38.Dennis G, Sherman BT, Hosack DA, Yang J, Gao W, Lane HC, Lempicki RA. DAVID: Database for Annotation, Visualization, and Integrated Discovery. Genome biology 2003; 4:P3.
39.Rose PW, Prlić A, Altunkaya A, Bi C, Bradley AR, Christie CH, Costanzo LD, Duarte JM, Dutta S, Feng Z, Green RK, Goodsell DS, Hudson B, Kalro T, Lowe R, Peisach E, Randle C, Rose AS, Shao C, Tao Y-P, Valasatava Y, Voigt M, Westbrook JD, Woo J, Yang H, Young JY, Zardecki C, Berman HM, Burley SK. The RCSB protein data bank: integrative view of protein, gene and 3D structural information. Nucleic acids research 2017; 45:D271-D281.
40.Trott O, Olson AJ. AutoDock Vina: improving the speed and accuracy of docking with a new scoring function, efficient optimization, and multithreading. Journal of computational chemistry 2010; 31:455-461.
41.Liu Y, Grimm M, Dai W-T, Hou M-C, Xiao Z-X, Cao Y. CB-Dock: a web server for cavity detection-guided protein-ligand blind docking. Acta pharmacologica Sinica 2020; 41:138-144.
42.Miao J, Ye S, Lan J, Ye P, Wen Q, Mei L, Liu X, Lin J, Zhou X, Du S, Liu X, Li H. Nuclear HMGB1 promotes the phagocytic ability of macrophages. Exp Cell Res 2020; 393:112037.
43.Yin C, Hu W, Wang M, Lv W, Jia T, Xiao Y. Irisin as a mediator between obesity and vascular inflammation in Chinese children and adolescents. Nutr Metab Cardiovasc Dis 2020; 30:320-329.
44.Kelly DP. Medicine. Irisin, light my fire. Science (New York, NY) 2012; 336:42-43.
45.Huerta-Delgado AS, Roffe-Vazquez DN, Gonzalez-Gil AM, Villarreal-Calderon JR, Tamez-Rivera O, Rodriguez-Gutierrez NA, Castillo EC, Silva-Platas C, Garcia-Rivas G, Elizondo-Montemayor L. Serum Irisin Levels, Endothelial Dysfunction, and Inflammation in Pediatric Patients with Type 2 Diabetes Mellitus and Metabolic Syndrome. J Diabetes Res 2020; 2020:1949415.
46.Lourenco MV, Frozza RL, de Freitas GB, Zhang H, Kincheski GC, Ribeiro FC, Goncalves RA, Clarke JR, Beckman D, Staniszewski A, Berman H, Guerra LA, Forny-Germano L, Meier S, Wilcock DM, de Souza JM, Alves-Leon S, Prado VF, Prado MAM, Abisambra JF, Tovar-Moll F, Mattos P, Arancio O, Ferreira ST, De Felice FG. Exercise-linked FNDC5/irisin rescues synaptic plasticity and memory defects in Alzheimer's models. Nat Med 2019; 25:165-175.
47.Narayanan SA, Metzger CE, Bloomfield SA, Zawieja DC. Inflammation-induced lymphatic architecture and bone turnover changes are ameliorated by irisin treatment in chronic inflammatory bowel disease. FASEB J 2018; 32:4848-4861.
48.Pedersen BK, Saltin B. Evidence for prescribing exercise as therapy in chronic disease. Scandinavian journal of medicine & science in sports 2006; 16 Suppl 1:3-63.
49.Madkour MM, Anbar HS, El-Gamal MI. Current status and future prospects of p38α/MAPK14 kinase and its inhibitors. European journal of medicinal chemistry 2021; 213:113216.

50.Wan Y, Chong L-W, Evans RM. PPAR-gamma regulates osteoclastogenesis in mice. Nature medicine 2007; 13:1496-1503.
51.Zhu W, Yan H, Li S, Nie W, Fan F, Zhu J. PPAR-γ agonist pioglitazone regulates dendritic cells immunogenicity mediated by DC-SIGN via the MAPK and NF-κB pathways. International immunopharmacology 2016; 41:24-34.
52.Lei W, Li X, Li L, Huang M, Cao Y, Sun X, Jiang M, Zhang B, Zhang H. Compound Danshen Dripping Pill ameliorates post ischemic myocardial inflammation through synergistically regulating MAPK, PI3K/AKT and PPAR signaling pathways. J Ethnopharmacol 2021; 281:114438.
53.Mirza AZ, Althagafi, II, Shamshad H. Role of PPAR receptor in different diseases and their ligands: Physiological importance and clinical implications. Eur J Med Chem 2019; 166:502-513.
54.Liu WX, Wang T, Zhou F, Wang Y, Xing JW, Zhang S, Gu SZ, Sang LX, Dai C, Wang HL. Voluntary exercise prevents colonic inflammation in high-fat diet-induced obese mice by up-regulating PPAR-gamma activity. Biochem Biophys Res Commun 2015; 459:475-480.
55.Bertin B, Dubuquoy L, Colombel J-F, Desreumaux P. PPAR-gamma in ulcerative colitis: a novel target for intervention. Current drug targets 2013; 14:1501-1507.
56.Decara J, Rivera P, Lopez-Gambero AJ, Serrano A, Pavon FJ, Baixeras E, Rodriguez de Fonseca F, Suarez J. Peroxisome Proliferator-Activated Receptors: Experimental Targeting for the Treatment of Inflammatory Bowel Diseases. Front Pharmacol 2020; 11:730.
57.Wang L, Xie H, Xu L, Liao Q, Wan S, Yu Z, Lin D, Zhang B, Lv Z, Wu Z, Sun X. rSj16 Protects against DSS-Induced Colitis by Inhibiting the PPAR-α Signaling Pathway. Theranostics 2017; 7:3446-3460.
58.Zakaria R, Yaacob WMW, Othman Z, Long I, Ahmad AH, Al-Rahbi B. Lipopolysaccharide-induced memory impairment in rats: a model of Alzheimer's disease. Physiological research 2017; 66:553-565.
59.Dat LD, Thao NP, Tai BH, Luyen BTT, Kim S, Koo JE, Koh YS, Cuong NT, Thanh NV, Cuong NX, Nam NH, Kiem PV, Minh CV, Kim YH. Chemical constituents from Kandelia candel with their inhibitory effects on pro-inflammatory cytokines production in LPS-stimulated bone marrow-derived dendritic cells (BMDCs). Bioorganic & medicinal chemistry letters 2015; 25:1412-1416.
60.Wei WC, Liu CP, Yang WC, Shyur LF, Sheu JH, Chen SS, Yang NS. Mammalian target of rapamycin complex 2 (mTORC2) regulates LPS-induced expression of IL-12 and IL-23 in human dendritic cells. J Leukoc Biol 2015; 97:1071-1080.
61.Brereton CF, Sutton CE, Lalor SJ, Lavelle EC, Mills KH. Inhibition of ERK MAPK suppresses IL-23- and IL-1-driven IL-17 production and attenuates autoimmune disease. J Immunol 2009; 183:1715-1723.
62.Dobreva ZG, Stanilova SA, Miteva LD. The influence of JNK and P38 MAPK inhibition on IL-12P40 and IL-23 production depending on IL12B promoter polymorphism. Cell Mol Biol Lett 2009; 14:609-621.
63.Lin CH, Yeh SH, Lin CH, Lu KT, Leu TH, Chang WC, Gean PW. A role for the PI-3 kinase signaling pathway in fear conditioning and synaptic plasticity in the amygdala. Neuron 2001; 31:841-851.
64.Edström A, Ekström PAR. Role of phosphatidylinositol 3-kinase in neuronal survival and axonal outgrowth of adult mouse dorsal root ganglia explants. Journal of neuroscience research 2003; 74:726-735.
65.Huang XL, Xu J, Zhang XH, Qiu BY, Peng L, Zhang M, Gan HT. PI3K/Akt signaling pathway

is involved in the pathogenesis of ulcerative colitis. Inflamm Res 2011; 60:727-734.
66.Cao X, Fu M, Bi R, Zheng X, Fu B, Tian S, Liu C, Li Q, Liu J. Cadmium induced BEAS-2B cells apoptosis and mitochondria damage via MAPK signaling pathway. Chemosphere 2021; 263:128346.
67.Wang G, Xu B, Shi F, Du M, Li Y, Yu T, Chen L. Protective Effect of Methane-Rich Saline on Acetic Acid-Induced Ulcerative Colitis via Blocking the TLR4/NF-kappaB/MAPK Pathway and Promoting IL-10/JAK1/STAT3-Mediated Anti-inflammatory Response. Oxid Med Cell Longev 2019; 2019:7850324.
68.Gao W, Wang C, Yu L, Sheng T, Wu Z, Wang X, Zhang D, Lin Y, Gong Y. Chlorogenic Acid Attenuates Dextran Sodium Sulfate-Induced Ulcerative Colitis in Mice through MAPK/ERK/JNK Pathway. Biomed Res Int 2019; 2019:6769789.
69.Setia S, Nehru B, Sanyal SN. Upregulation of MAPK/Erk and PI3K/Akt pathways in ulcerative colitis-associated colon cancer. Biomed Pharmacother 2014; 68:1023-1029.
70.Schwanke RC, Marcon R, Meotti FC, Bento AF, Dutra RC, Pizzollatti MG, Calixto JB. Oral administration of the flavonoid myricitrin prevents dextran sulfate sodium-induced experimental colitis in mice through modulation of PI3K/Akt signaling pathway. Mol Nutr Food Res 2013; 57:1938-1949.
71.Bai X, Gou X, Cai P, Xu C, Cao L, Zhao Z, Huang M, Jin J. Sesamin Enhances Nrf2-Mediated Protective Defense against Oxidative Stress and Inflammation in Colitis via AKT and ERK Activation. Oxid Med Cell Longev 2019; 2019:2432416.

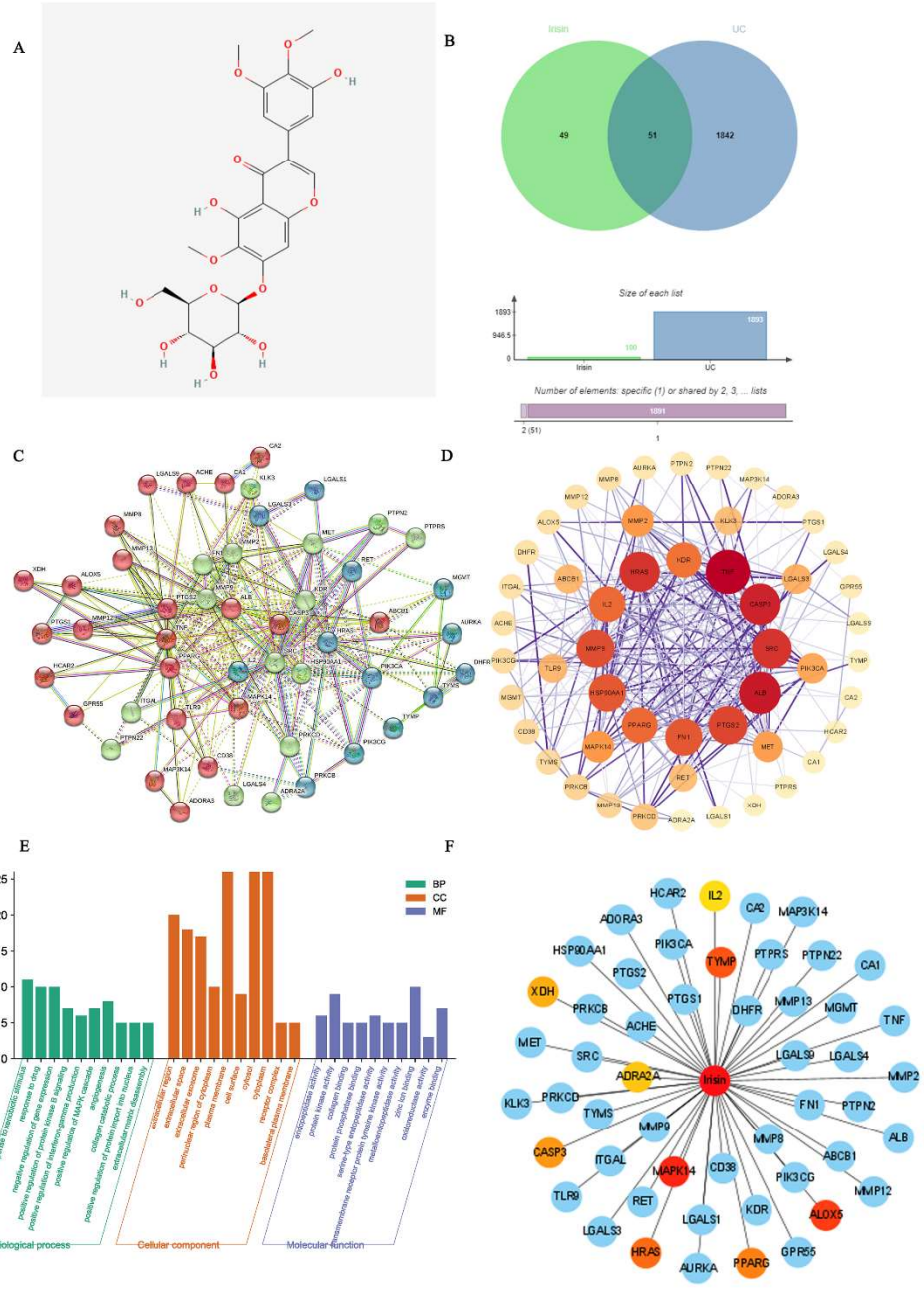

Fig.1. Candidate targets and PPI network construction. A, The structure of irisin. B, A Venn map shows the targets that irisin intersects with UC. C, The PPI networks. D, import the CSV format result file of PPI into Cytoscape 3.9.1 for visualization. High-degree nodes are larger and closer to red, while low-degree nodes are smaller and closer to yellow. E, GO enrichment analysis. The Y-axis shows the enriched count and the X-axis shows significantly enriched GO terms of the intersectional targets. F, Component-target network of irisin.

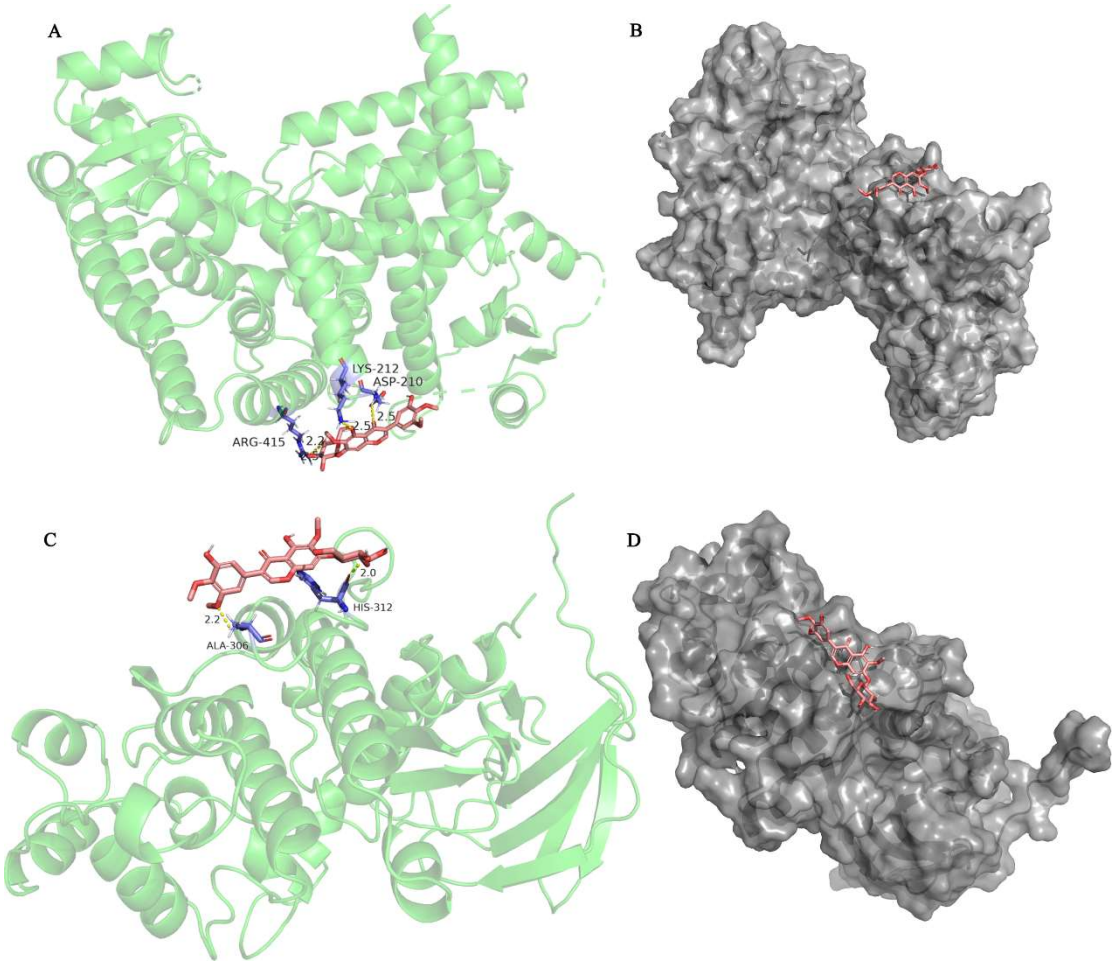

Fig.2. The docking model of irisin with PPAR γ and MAPK14 respectively. The action model of PPAR γ with irisin. B, Binding pocket construction of PPAR γ with irisin. C, The action model of MAPK14 with irisin. D, Binding pocket construction of MAPK14 with irisin. The hydrogen bonds were indicated by dashed lines and the length was added around the lines.

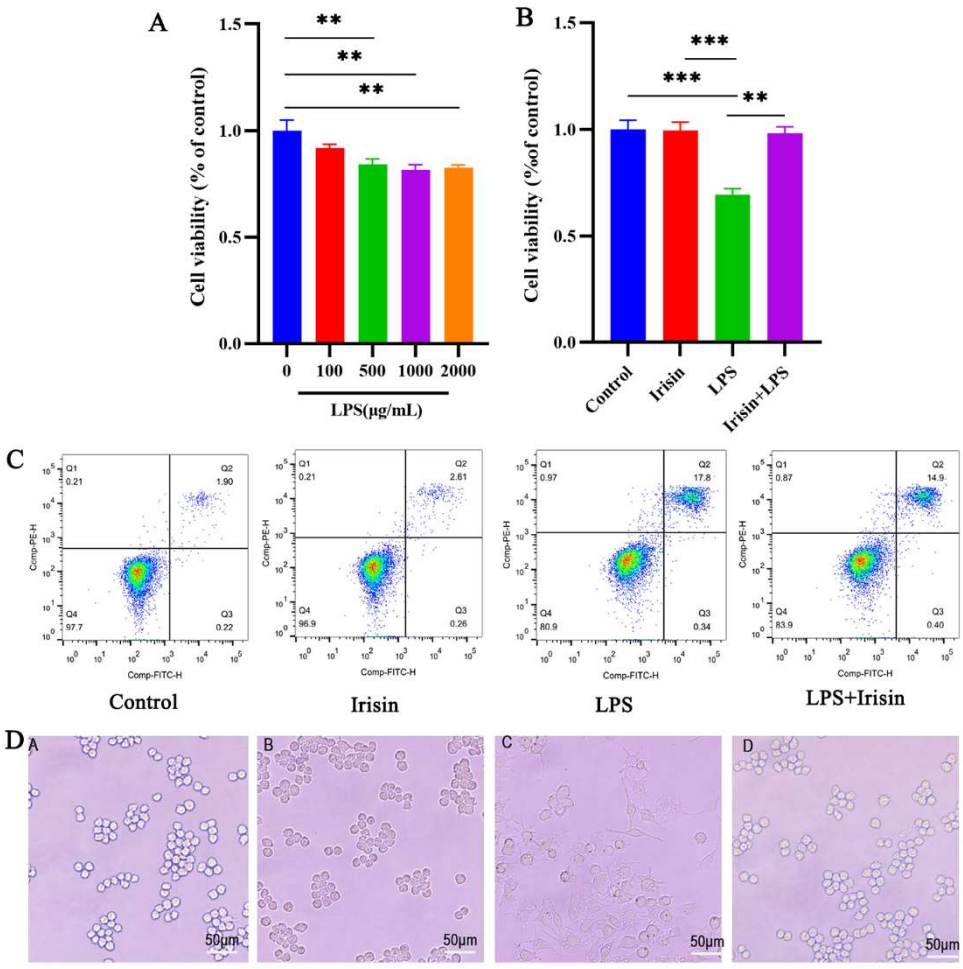

Fig.3. Irisin protected RAW264.7 from LPS-induced cell injury. An MTT assay showed RAW264.7 cells viability at different concentrations of LPS. B, Protective effects of irisin pretreatment on LPS-stimulated macrophage RAW 264.7 cells. Irisin pretreatment reverses the cell injury induced by LPS. C, Protective of irisin pretreatment on LPS-induced apoptotic of macrophage. RAW264.7 macrophages were divided into four groups, treated with culture medium, irisin (400 ng/ml), and LPS (1000 ng/ml) alone for 24h, after pretreatment with irisin for 12h, LPS was added for 12h, described in the "Materials and Methods" section. The total percentage of apoptosis is equal to the percentage of early apoptosis (Q2) plus the percentage of late apoptosis (Q3). Representative images from flow cytometry. D, The effect of irisin or LPS on the morphology of RAW264.7 macrophages. Cells were cultured with medium (A), irisin (400ng/ml) (B), or LPS (1000ng/ml) (C), respectively, or cells were pretreated with irisin for 12 hours, and then LPS was added (D). The cell morphology was determined using an optical microscope (400 ×). Data presented as mean ±SE (n = 3). ** *P*<

0.01, *** $P < 0.001$. Control, medium; Irisin, 400ng/ml irisin; LPS, 1000 ng/ml LPS; Irisin + LPS: after pretreatment with irisin (400 ng/ml) for 12h, LPS (1000 ng/ml) was added for 12h.

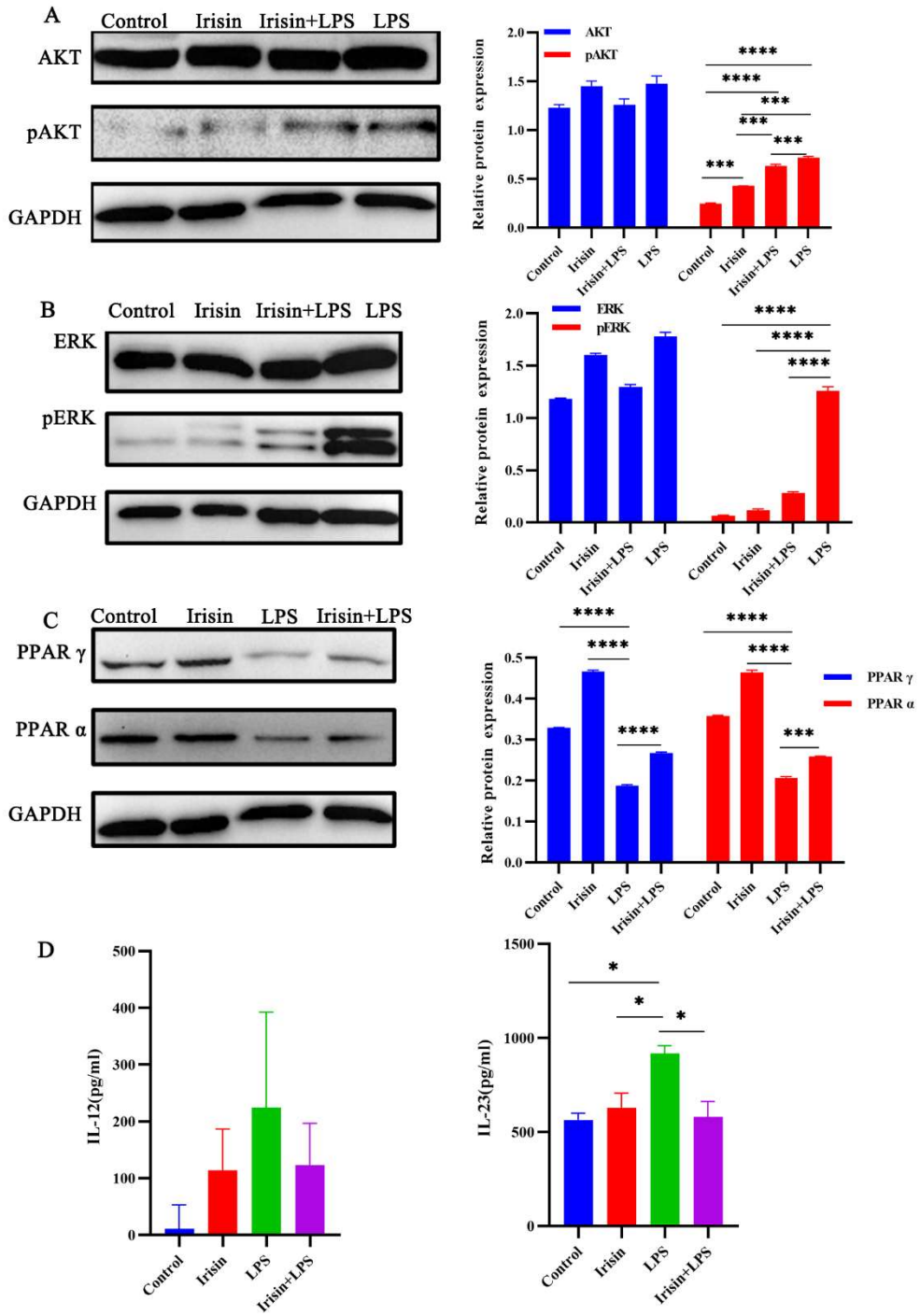

Fig.6. RAW264.7 were treated with medium, irisin (400ng/ml), or LPS (1000ng/ml) for 24h, respectively, or after pretreatment for 12h, LPS was added for 12h, and then were collected to determine the expression of ERK, pERK, AKT, pAKT, PPAR α, and PPAR γ by Western blot assay described as the "Materials and Methods" section. A. Influence of irisin and LPS on the protein

expression levels of AKT, pAKT, and densitometric quantification normalized to GAPDH. B, Influence of irisin and LPS on the protein expression levels of ERK, pERK, and densitometric quantification normalized to GAPDH. C, Influence of irisin and LPS on the protein expression levels of PPAR α, PPAR γ and densitometric quantification normalized to GAPDH. D, for cytokine protein determination, RAW264.7were treated with medium, irisin (400ng/ml), and LPS (1000ng/ml) for 24h respectively, or after pretreatment with irisin for 12h, LPS was added for 12h, then cell-free supernatants were collected and assessed for IL-12 and IL-23 production by ELISA. Data presented as mean ± SE (n = 3). *P< 0.05, *** P< 0.001, **** P< 0.0001. Control, medium; Irisin, 400ng/ml irisin; LPS, 1000 ng/ml LPS; Irisin + LPS: after pretreatment with irisin (400 ng/ml) for 12h, LPS (1000 ng/ml) was added for 12h.

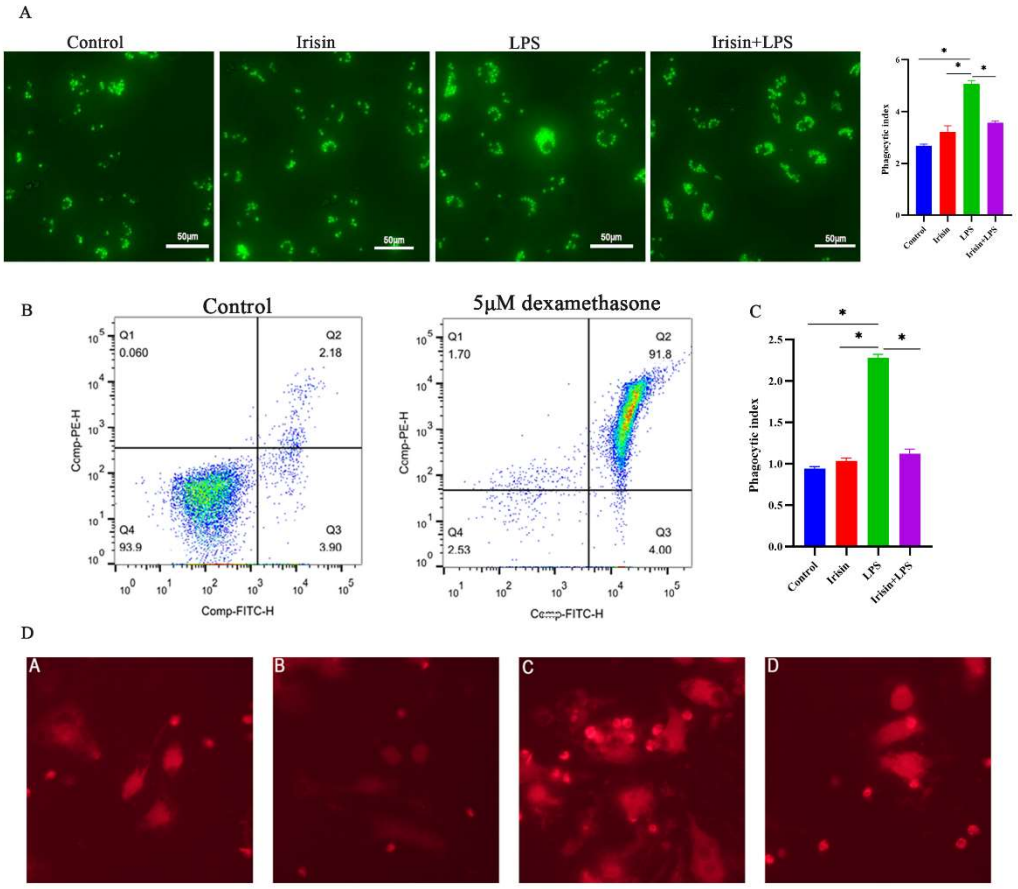

Fig.5. A, Zymosan Phagocytosis in RAW264.7 macrophage. 10^5 Macrophages were cultured in a medium, irisin (400ng/ml), and LPS (1000ng/ml) alone respectively, or pre-treated for 12 h with irisin, and then LPS were added for 12h. Phagocytosis was allowed to proceed for 30min. For 30 minutes at 4°C, cells were fixed with 4% paraformaldehyde, followed by a PBS wash. Using a Nikon Eclipse Ti2-E microscope, the plate was analyzed using light microscopy at 400x magnification. B, Dead cell clearance by macrophages. For the dead cell clearance assay, macrophages were co-cultured with a cell tracker labeled (red) thymocytes. Over 90% of cells become phosphatidylserine positive after incubation with 5μM dexamethasone. C, scoring of thymocytes engulfed by macrophage. D, Apoptotic thymocytes (red) engulfed by macrophages. Data presented as mean ± SE (n = 3). *P< 0.05. Control, medium; Irisin, 400ng/ml irisin; LPS, 1000 ng/ml LPS; Irisin + LPS: after pretreatment with irisin (400 ng/ml) for 12h, LPS (1000 ng/ml) was added for 12h.

Table S1. Common target information for Irisin and UC

Table S2. Information on the PPI network

Table S3. Information on GO enrichment analysis